ACS OMEGA

Open Access

http://pubs.acs.org/journal/acsodf

Article

Experimental Study of Compatibility between the Eco-friendly Insulation Mixed Gas CF_3SO_2F/N_2 and EPDM and CR Materials

Wei Liu, Yu Zheng,* Wenliang Zhang, Fengxiang Ma, Zilin Tao, Yuzheng Guo, and Wenjun Zhou*

Cite This: *ACS Omega* 2024, 9, 7958−7966

Read Online

ACCESS | Metrics & More | Article Recommendations

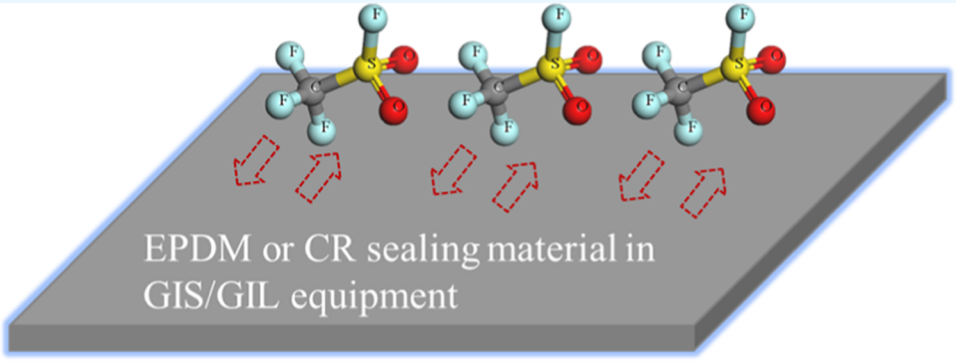

ABSTRACT: As a greenhouse gas with strong global warming potential, the use of SF_6 needs to be reduced as much as possible. Researching environmentally friendly insulation (EFI) gases to replace SF_6 in power electrical equipment is an effective way to reduce its usage. CF_3SO_2F/N_2, as a newly proposed EFI gas, has certain potential to replace SF_6. Compatibility of CF_3SO_2F/N_2 gas with rubber sealing materials commonly used in electrical equipment is still unknown. In this article, the compatibility of CF_3SO_2F/N_2 with the ethylene-propylene-diene monomer (EPDM) and chloroprene rubber (CR) was investigated experimentally. It was found that CF_3SO_2F/N_2 would slightly decompose under the influence of EPDM and CR rubber under certain conditions. The surface morphology of EPDM changed slightly under the influence of CF_3SO_2F/N_2, and it was similar to the influence of SF_6. While the surface morphology of CR deteriorated significantly with obvious defects. The mechanical properties of EPDM were not significantly affected by CF_3SO_2F, which is similar to the influence of SF_6. But CR was affected greatly by CF_3SO_2F gas. Permanent deformation compression and surface morphology are two effective indicators for characterizing the compatibility between gas and rubber sealing materials. This research provides a reference for the application of CF_3SO_2F/N_2 as a new EFI gas in power equipment.

INTRODUCTION

SF_6 gas is widely used in gas-insulated electrical equipment (GIE) because of its excellent insulating properties and arc extinguishing ability.[1,2] However, SF_6 is also a greenhouse gas with the strongest greenhouse effect. According to IPCC's Sixth Assessment Report Climate Change, SF_6 has an atmospheric lifetime of 1000 years and a global warming potential (GWP) of 24,300.[3] This means that every 1 kg of SF_6 emitted is equivalent to 24.3 tons of CO_2 emitted. Therefore, the development of environment-friendly insulation (EFI) gases to replace SF_6 has become an important and hot research issue in the power electrical industry.[4,5]

CF_3SO_2F is a newly proposed EFI gas with huge potential to replace SF_6. According to existing studies, its dielectric strength is about 40% higher than that of SF_6, and its GWP is 86% lower than SF_6. Moreover, the liquefaction temperature of CF_3SO_2F at 0.1 MPa is about −23 °C, much lower than existing EFI gases such as C_4F_7N, $C_5F_{10}O$, etc.[6,7] When it is mixed with N_2 or CO_2 at higher pressures, the synergistic effect of the CF_3SO_2F/N_2 mixture is better than that of CF_3SO_2F/CO_2, indicating that the CF_3SO_2F/N_2 mixture is more suitable for high-voltage GIE.[8] It is previously found that the 40% CF_3SO_2F/60% N_2 gas mixture can achieve equal insulation strength with SF_6.[9]

However, in addition to the insulating properties of CF_3SO_2F/N_2 gas, it is also necessary to consider the material compatibility between gases and solid materials when considering the use of CF_3SO_2F/N_2 gas.[10−12] As sealing

Received: October 11, 2023
Revised: December 10, 2023
Accepted: January 25, 2024
Published: February 6, 2024

materials in the GIE, current rubber materials should be compatible with CF_3SO_2F/N_2 gas. Otherwise, it may cause gas leakage and cause insulation breakdown accidents. Therefore, investigation is needed to investigate the compatibility between CF_3SO_2F/N_2 and rubber materials commonly used in GIE.

In recent years, researchers at home and abroad have carried out in-depth studies of the compatibility between various EFI gases and rubber materials. Zheng et al. found that the chemical reaction between C_4F_7N gas and ethylene-propylene-diene monomer (EPDM) occurs under the thermal acceleration test.[13] Cheng et al. found that $C_5F_{10}O$ decomposes into gases such as C_3F_6O, C_3F_6, and C_3HF_7 after the thermal acceleration test, and the rubber itself is also embrittled.[14] Lan et al. investigated the compatibility between the $C_6F_{12}O/N_2$ gas mixture and nitrile rubber and found that the two undergo a strong chemical reaction at high temperatures.[15] Wu et al. investigated the compatibility between the $C_4F_7N/CO_2/O_2$ ternary gas mixture and EPDM and found that O_2 exacerbates the reaction between C_4F_7N and EPDM.[16] Wang et al. studied the compatibility of C_4F_7N/CO_2 and its decomposition gases with rubber materials and found that nitrile rubber is less compatible with C_4F_7N/CO_2.[17] From the above research, it can be seen that the study of compatibility plays an important role in the practical application of EFI gases; therefore, it is necessary to carry out research on compatibility between CF_3SO_2F gas and rubber sealing materials.

The compatibility between CF_3SO_2F/N_2 gas and two kinds of rubber, EPDM, and chloroprene rubber (CR), which are commonly used in GIE, is studied by a thermal acceleration experiment. The compatibility between those two is evaluated by the decomposition of CF_3SO_2F/N_2 gas under the influence of rubber and the performance deterioration of rubber under the influence of CF_3SO_2F/N_2 gas. Experimental results could provide compatibility perspective evidence for evaluating the feasibility of CF_3SO_2F/N_2 gas as one of the SF_6 alternatives.

EXPERIMENTAL METHOD

Preparation of Samples. Due to the problem of liquefaction of pure CF_3SO_2F gas at high pressures, a mixture of CF_3SO_2F/N_2 was selected for the test. The mole ratio of CF_3SO_2F at 40% was used, which can make the insulation strength of the CF_3SO_2F/N_2 mixture equivalent to that of SF_6. A control group using SF_6 gas was also studied. The CF_3SO_2F gas used in this study was supplied by Beijing Yuji Co. with a purity of 99%. N_2 and SF_6 gases were conventional commercial supplies with a purity higher than 99.99%.

The rubber materials used in this study were EPDM and CR. They are commonly used sealing materials in high-voltage electrical equipment.[18] The rubber materials were provided by Henan Pinggao Electric Co. The rubber materials were prepared into corresponding tensile and compression samples for testing according to ISO 815-1 and ISO 37.[19,20] The dimensional drawings of the two specimens are shown in Figure 1.

Test Method. As a long-term indicator, compatibility is usually studied using the thermal acceleration test.[21] In this test, the chemical reaction rate is accelerated by increasing the temperature, thereby characterizing the aging condition of material under decades of service within an acceptable test time range. The selection of temperature is crucial in the thermal acceleration test. It is necessary to increase the temperature to simulate a sufficiently long operating time, but the temperature should not be too high to cause material

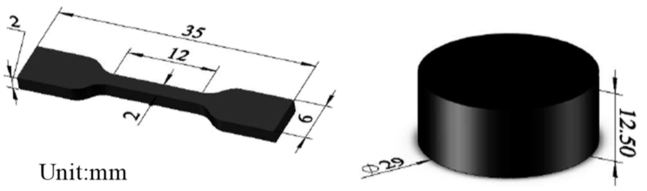

Figure 1. Dimensions of the rubber sample.

cracking. In this study, a gas−solid compatibility test platform was set up to carry out thermal acceleration tests using a metal-sealed container and a high-temperature test chamber. The composition and proportion of CF_3SO_2F/N_2 mixed gas after the test were detected by gas chromatography−mass spectrometry (GC−MS). The surface morphology of the rubber and the surface element after the test were detected by field emission scanning electron microscopy and energy-dispersive spectrometry. The mechanical properties of rubber after testing were detected by a universal testing machine. The compatibility of CF_3SO_2F/N_2 gas with EPDM and CR was determined by the above tests, as shown in Figure 2.

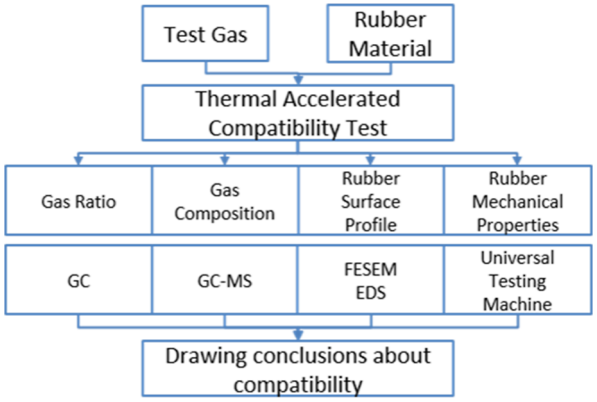

Figure 2. Compatibility test flowchart.

Test Conditions. To set a suitable thermal acceleration test temperature, we mainly referred to the ISO 23529:2004 and IEC 62271-1:2017.[22,23] For the selection of temperature gradient for comparison, the test temperature was selected at three temperature levels, namely 70, 85, and 100 °C.

To set the suitable test pressure for CF_3SO_2F/N_2 mixed gas, we referred to IEC 62271-200:2011. The gas pressure inside the compartment should be determined according to the manufacturer and the user.[24] Since CF_3SO_2F/N_2 has not yet been put into practical industrial applications, we referred to the current use of SF_6 gas-insulated equipment. The test pressure of CF_3SO_2F/N_2 was set at an absolute pressure of 0.4 MPa.[5] For the control group, SF_6 gas with an absolute pressure of 0.4 MPa was used. The test duration was selected as 7 days with reference to ISO 23529:2004. The compatibility between CF_3SO_2F/N_2 gas and two types of rubber was evaluated by detecting the decomposition of the gas under the influence of rubber and the chemical reaction of rubber under the influence of gas before and after the test.

RESULTS AND DISCUSSION

Gas Composition Changing Law. The gas−solid compatibility tests were performed using the test methods. After tests, the composition of CF_3SO_2F/N_2 gas mixture was

https://doi.org/10.1021/acsomega.3c07958
ACS Omega 2024, 9, 7958−7966

detected by GC−MS. The chromatographic column used was GS-GASPRO 60 m, and the inlet temperature was 100 °C. The total flow rate was 67.9 mL/min. The column flow rate was 3.09 mL/min. The linear velocity was 44.7 cm/s. The purging flow rate was 3 mL/min. The split ratio was 20:1. The heating program was controlled by an initial temperature of 35 °C, held for 5 min, then increased to 150 °C at a rate of 8 °C/min, and held for 10 min. The MS conditions were set at 200 °C for the ion source and 200 °C for the interface.

The results showed that the decomposition gas was generated at 70, 85, and 100 °C. The gas peaks of the decomposed gases were more obvious after the temperature was increased. Taking the GC−MS detection results of the gas at 100 °C as an example, Figures 3 and 4 show the GC−MS

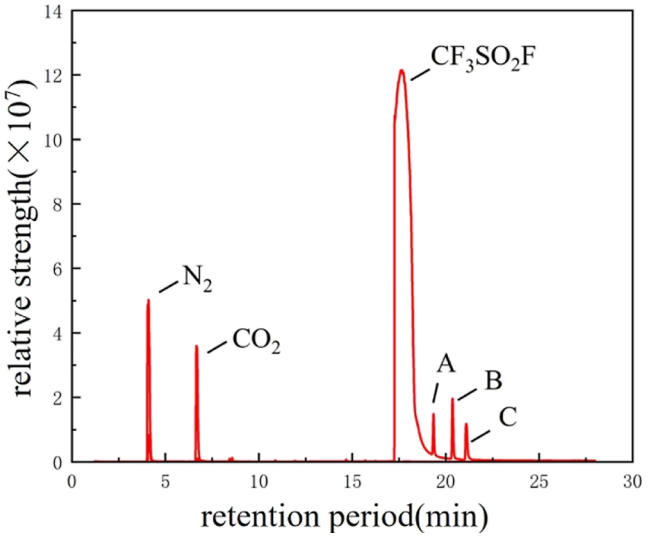

Figure 3. GC−MS results of EPDM and CF_3SO_2F/N_2 at 100 °C.

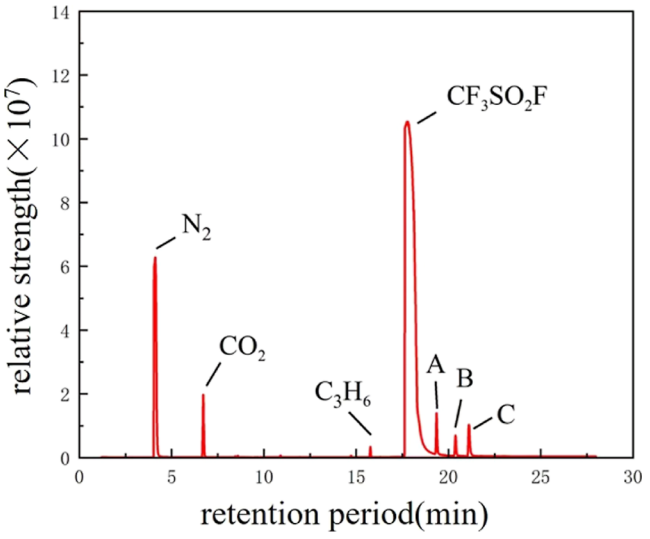

Figure 4. GC−MS results of CR and CF_3SO_2F/N_2 at 100 °C.

detection results of the gas after the test of EPDM and CR at 100 °C, respectively, which show that EPDM and CR will lead to the generation of decomposition gases after the test with CF_3SO_2F/N_2. The gases A−C in Figures 2 and 3 are $C_2F_6O_5S_2$, $C_2H_3ClF_2$, and CF_4, respectively. $C_2F_6O_5S_2$ may be formed by the combination of two CF_3SO_2F molecules after breakage of the S−F bond, and $C_2H_3ClF_2$ is formed after reacting with rubber. CF_4 may be formed due to the removal of the CF_3 group from CF_3SO_2F.

Comparing the results in Figures 5 and 6, it can be seen that no decomposition gases were detected after the compatibility

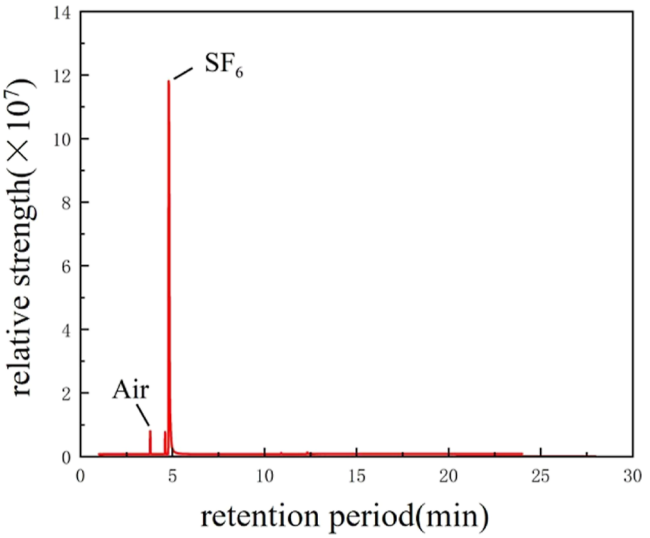

Figure 5. GC−MS test results of EPDM and SF_6 at 100 °C.

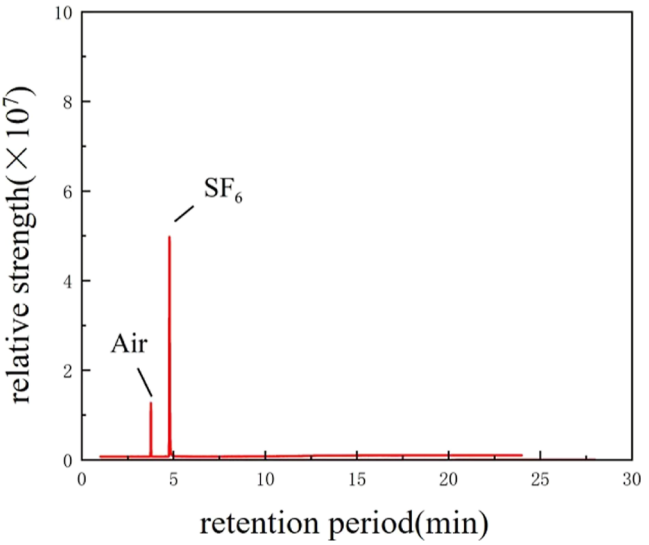

Figure 6. GC−MS test results of CR and SF_6 at 100 °C.

tests of SF_6 with EPDM and CR, which suggests that the rubber itself does not form decomposition gases under the same test conditions, and that the decomposition gases are due to the reaction between EPDM, CR, and CF_3SO_2F/N_2 at high temperatures. This indicates that there is a compatibility problem between CF_3SO_2F/N_2 and EPDM/CR. Tests at high temperatures show that decomposition gases formed between CF_3SO_2F/N_2 and rubber, which led to a decrease in the gas ratio of CF_3SO_2F and resulted in a decrease in its insulating ability.

Gas Ratio Changing Law. After the tests, the gas proportion of CF_3SO_2F was detected by GC, and the test results are shown in Table 1. It can be seen that for the effect of EPDM on the proportion of CF_3SO_2F, it decreased by 1.55% at 70 °C, 2.06% at 85 °C, and 5.61% at 100 °C. For the

https://doi.org/10.1021/acsomega.3c07958
ACS Omega 2024, 9, 7958−7966

Table 1. Mole Ratio of CF_3SO_2F before and after the Compatibility Test

test group	test temperature/°C	ratio before test/%	ratio after test/%
EPDM	70	39.38	37.83
	85	40.72	38.66
	100	40.69	35.08
CR	70	40.75	37.34
	85	40.06	36.94
	100	40.11	35.13

effect of CR on the proportion of CF_3SO_2F, it also decreased, with 3.41% at 70 °C, 3.12% at 85 °C, and 4.98% at 100 °C. The results show that the proportions of CF_3SO_2F after the compatibility test with CR are approximately the same as those of EPDM. This indicates that the effect of EPDM and CR on CF_3SO_2F/N_2 is nearly the same.

It also shows that the effect of both EPDM and CR on the proportion decrease of CF_3SO_2F becomes more obvious with the increase of the test temperature. The thermal acceleration test speeds up the reaction rate by increasing the temperature, thus reflecting in a short time what happens over a longer period of time. Therefore, the test results show that both EPDM and CR will cause a decrease in the gas proportion of CF_3SO_2F when coexisting with CF_3SO_2F for a long period of time.

Surface Morphology Changing Law. After the tests, the surface morphology of EPDM and CR was analyzed, as shown in Figure 7. At 70 °C, the surface of EPDM after testing with CF_3SO_2F/N_2 is seen to have some crystals precipitated. While

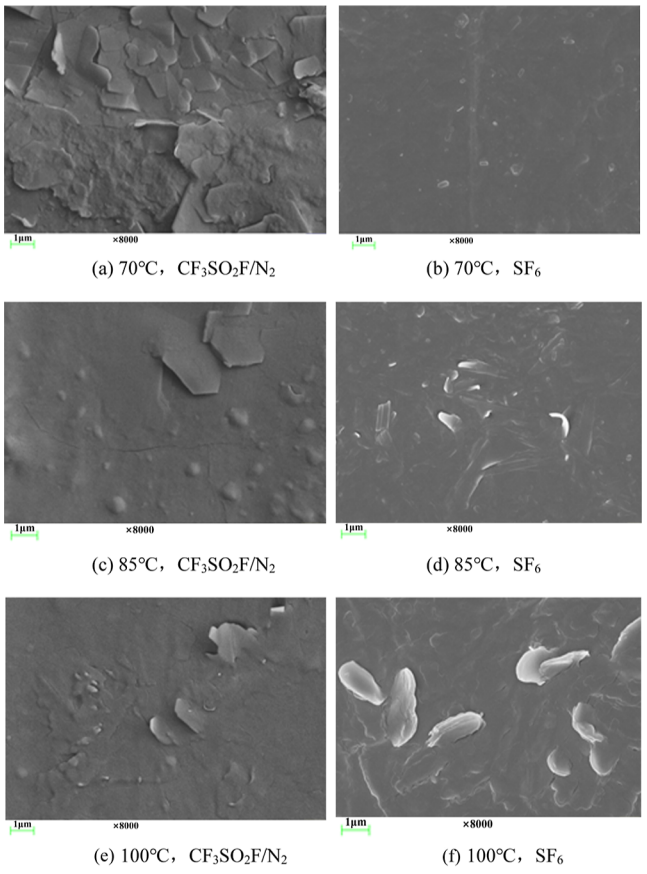

Figure 7. Surface morphology of EPDM after tests.

in the SF_6 control group, the surface morphology of EPDM is more smooth without obvious defects. The surface of EPDM is seen to have some crystals precipitated in both the test group with CF_3SO_2F/N_2 and the control group with SF_6 at 85 and 100 °C. It is seen that the erosion of CF_3SO_2F/N_2 on the surface of EPDM is similar to the erosion of SF_6 on the surface of EPDM.

The surface morphology of CR after tests is shown in Figure 8. It is seen that the surface morphology of CR in $CF_3SO_2F/$

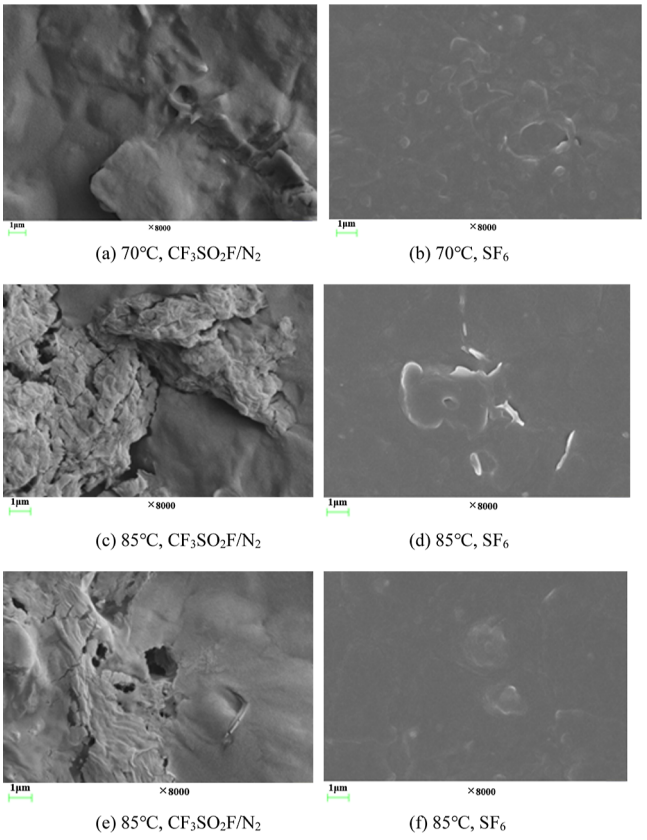

Figure 8. Surface morphology of CR after tests.

N_2 at 70 °C has obvious unevenness, while there is no obvious phenomenon in the control group with SF_6. At 85 °C, CR in CF_3SO_2F/N_2 shows obvious cracks and defects on the surface, while the surface of CR in SF_6 is still intact. At 100 °C, CR in CF_3SO_2F/N_2 shows pits on the surface, but the CR in the control group still shows no obvious defects. This indicates that the erosion of CR by CF_3SO_2F/N_2 is significantly higher than that in the control group.

In addition, the surface elements of EPDM and CR were analyzed, and the elemental content on the rubber surface was detected using the point scanning method. The surface elemental contents of EPDM with CF_3SO_2F/N_2 and SF_6 after thermal acceleration tests are shown in Tables 2 and 3, respectively. Seven elements, namely C, O, Al, Si, S, Ca, and Zn, were detected on the surface of EPDM in the SF_6 control group. Among them, C is the element in the main chain of EPDM rubber. O, Al, Ca, and Zn are some metal oxide additives added to the rubber in the production process. S comes from vulcanizing agents, and Si comes from SiO_2 reinforcing agents. In the CF_3SO_2F/N_2 test group, it can be clearly seen that in addition to the seven elements detected in the control group, three elements were also detected, namely,

https://doi.org/10.1021/acsomega.3c07958
ACS Omega 2024, 9, 7958−7966

Table 2. Surface Elemental Content after Tests of EPDM and CF_3SO_2F/N_2

element	70 °C test group/%	85 °C test group/%	100 °C test group/%
C	94.99	96.10	95.59
O	3.45	2.63	2.45
F	0.30	0.48	0.72
Na	0.12		0.10
Al	0.08	0.09	0.07
Si	0.15	0.13	0.13
S	0.21	0.00	0.16
Cl		0.06	0.06
Ca	0.45	0.23	0.48
Zn	0.25	0.27	0.21

Table 3. Surface Elemental Content after Tests of EPDM and SF_6

element	70 °C test group/%	85 °C test group/%	100 °C test group/%
C	92.06	92.13	90.00
O	6.24	5.24	6.22
Al		0.25	0.16
Si	0.43	0.40	
S	0.00	0.50	1.09
Ca		0.82	1.76
Zn	1.26	0.66	0.77

Table 4. Surface Elemental Content after Tests of CR and CF_3SO_2F/N_2

element	70 °C test group/%	85 °C test group/%	100 °C test group/%
C	90.41	83.95	80.74
O	4.09	7.14	8.76
F	1.04	3.69	4.99
Na	0.14	0.15	0.14
Mg	0.46	1.21	1.18
Al	0.09	0.08	0.09
S	0.56	1.06	1.28
Cl	2.84	2.24	2.37
Ca	0.16	0.15	0.09
Fe		0.07	0.07
Zn	0.21	0.25	0.30

Table 5. Surface Elemental Content after Tests of CR and SF_6

element	70 °C test group/%	85 °C test group/%	100 °C test group/%
C	86.08	85.86	84.60
O	5.67	5.76	7.15
Mg	0.26	0.35	0.29
Al	0.22	0.12	0.13
S	0.50	0.50	
Cl	6.07	6.36	7.27
Ca		0.29	
Zn	1.20	0.76	0.57

F, Na, and Cl. Na is also likely to come from the metal oxide additives contained in the rubber itself. The small amount of Cl detected may be due to the Cl impurities in the test gas adhering to the rubber surface or reacting with the rubber. The source of element F, which was not included in the control group, was CF_3SO_2F gas. This suggests that a chemical reaction between CF_3SO_2F and EPDM has occurred, resulting in the detection of the element F attached to the surface of EPDM.

The surface elemental contents of CR with CF_3SO_2F/N_2 and SF_6 after tests are shown in Tables 4 and 5. It is seen that the element F was not detected in the control group but detected in the test group with CF_3SO_2F/N_2. This also indicates that chemical reactions between CF_3SO_2F and CR occurred, resulting in the attachment of the element F on the rubber surface.

The results of surface morphology tests showed that the surface morphology degradation of EPDM affected by CF_3SO_2F erosion was similar to that of SF_6, whereas CR was more severely affected by CF_3SO_2F erosion than by SF_6. Surface elemental tests also showed that both EPDM and CR are chemically reactive with CF_3SO_2F. The compatibility between EPDM and CF_3SO_2F is better than that of CR in terms of changes in rubber surface morphology.

https://doi.org/10.1021/acsomega.3c07958
ACS Omega 2024, 9, 7958−7966

Mechanical Properties Changing Law. Mechanical properties of rubber can reflect its sealing properties. The tensile and compression properties of the rubber materials were measured in this study. Figures 9 and 10 show the change

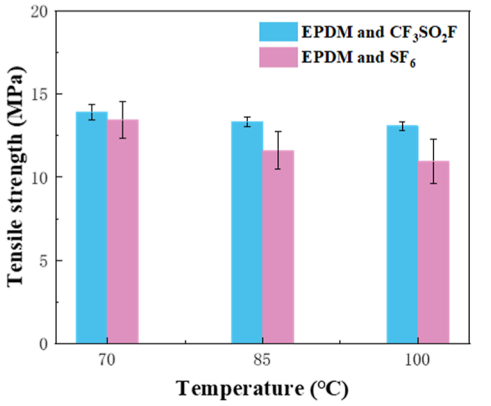

(a) tensile strength

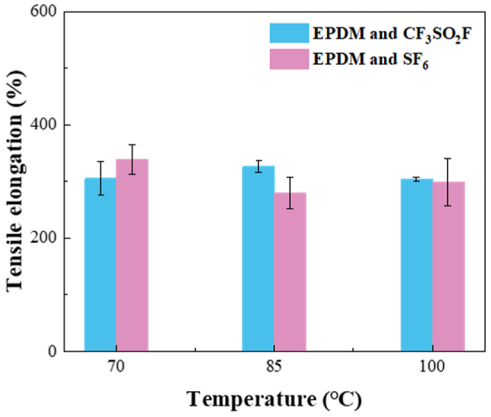

(b) tensile elongation

Figure 9. Tensile property of EPDM after the tests.

in tensile properties of EPDM and CR affected by CF_3SO_2F/N_2 and SF_6. It can be seen from Figure 9 that the tensile strength of EPDM in the CF_3SO_2F/N_2 gas is higher than that in SF_6. The tensile elongation of EPDM did not change significantly with temperature increase. Moreover, there is no obvious difference between the change of tensile elongation of EPDM in CF_3SO_2F/N_2 and that in SF_6. This indicates that the tensile properties of EPDM are less affected by CF_3SO_2F and similar to that in SF_6.

It can be seen from Figure 10 that the tensile strength of CR in CF_3SO_2F/N_2 gas decreases slightly with an increase of temperature. The tensile strength of CR in CF_3SO_2F/N_2 is higher than that in SF_6 at 70 °C, and the gap is gradually narrowed with the increase of temperature. There is also no obvious difference between the change in tensile elongation of CR in CF_3SO_2F/N_2 and that in SF_6. It can be seen that the tensile property of EPDM and CR does not deteriorate significantly under the influence of CF_3SO_2F. The tensile property of EPDM and CR under the influence of CF_3SO_2F is similar to that under SF_6 influence.

Figures 11 and 12 show the changes in compression properties of EPDM and CR under the influence of CF_3SO_2F and SF_6. Permanent deformation compression (PDC) and stiffness at 25% deformation are two main indicators of the

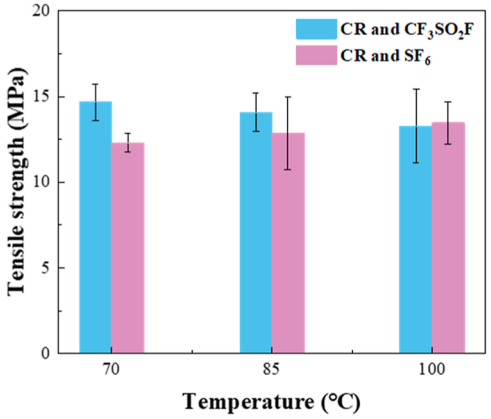

(a) tensile strength

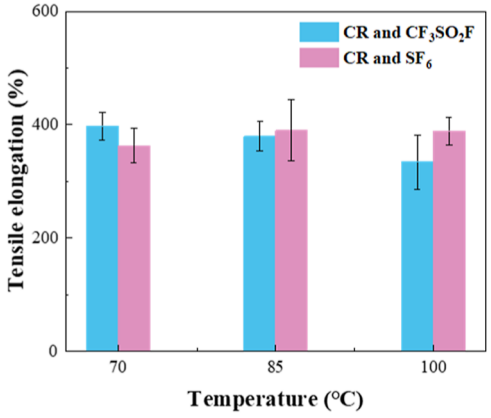

(b) tensile elongation

Figure 10. Tensile property of CR after the tests.

compression performance of rubber materials. As shown in Figure 11, the PDC of EPDM in CF_3SO_2F/N_2 and SF_6 gas both increased gradually with temperature. But the gap of PDC of EPDM in CF_3SO_2F/N_2 and SF_6 is small. It is seen from Figure 11 that the stiffness at 25% deformation of EPDM does not change much with temperature. The influence of CF_3SO_2F on the stiffness at 25% deformation of EPDM is also similar to that of SF_6.

As shown in Figure 12, the PDC of CR in CF_3SO_2F/N_2 or SF_6 gas is significantly higher than that of EPDM, and the stiffness at 25% deformation of CR is significantly lower than that of EPDM. This indicates that the compression performance of CR is less better than EPDM. The PDC of CR in CF_3SO_2F/N_2 increases significantly with temperature, but the PDC of CR in SF_6 changes little with temperature. The stiffness at 25% deformation of CR in CF_3SO_2F/N_2 decreases significantly with temperature increase. But it changes little with temperature increase in SF_6 gas. This indicates that the compression performance of CR is greatly affected by CF_3SO_2F/N_2 gas, but it will not be affected by SF_6. The result corresponds well with the surface test results in Figure 8.

The tensile property of EPDM and CR in CF_3SO_2F/N_2 is similar to that in SF_6, and the effect of the temperature is not obvious. The PDC property of EPDM in CF_3SO_2F/N_2 is also similar to that in SF_6, but the PDC property is significantly affected by temperature changes. For rubber sealing materials, compression performance is the main performance to be concerned about, so it can be assumed that temperature is the

https://doi.org/10.1021/acsomega.3c07958
ACS Omega 2024, 9, 7958−7966

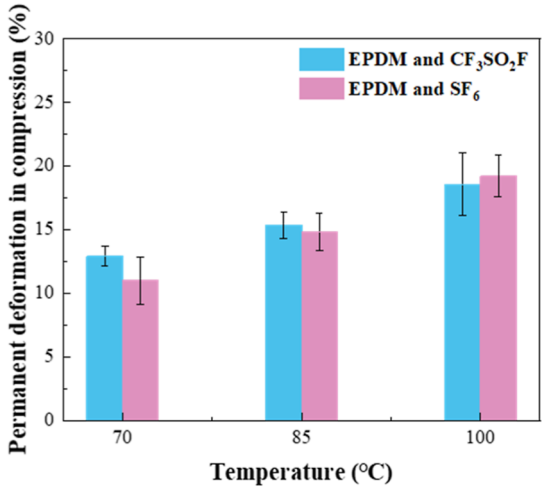

(a) permanent deformation compression

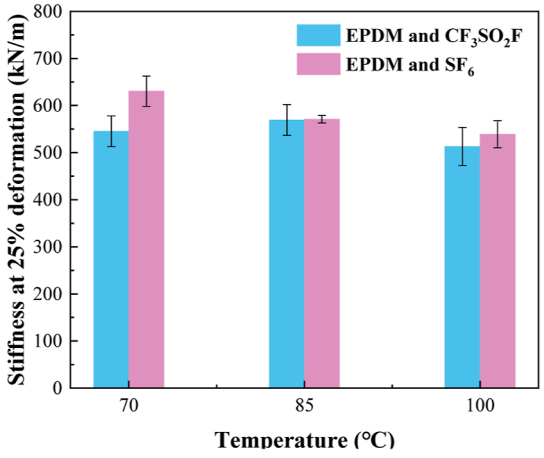

(b) stiffness at 25% deformation

Figure 11. Compression property of EPDM after the tests.

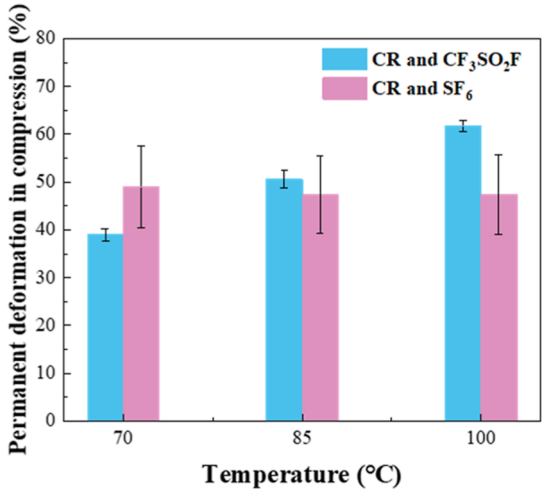

(a) permanent deformation compression

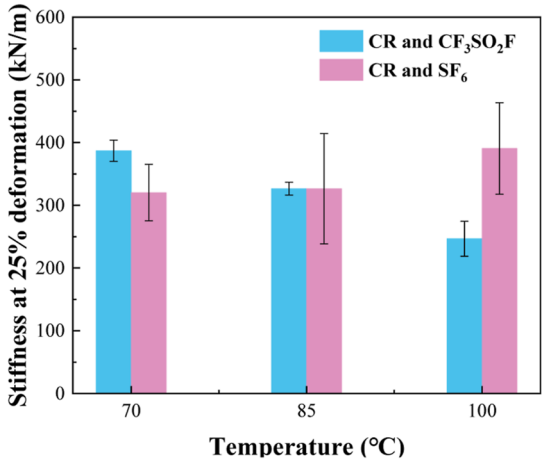

(b) stiffness at 25% deformation

Figure 12. Compression property of CR after the tests.

dominant influence on the mechanical properties of EPDM. However, for CR, the influence of CF_3SO_2F on the compression performance is not negligible. This may be due to a chemical reaction between CF_3SO_2F gas and the surface of CR rubber, which can be confirmed by the surface measurement results.

Discussion. Through previous experimental research, we can obtain the compatibility between the EFI gas CF_3SO_2F and the EPDM and CR rubber used in existing power equipment, which is of great significance for its practical engineering application. However, at the scientific level, it is usually more concerning what kind of reaction occurs between CF_3SO_2F and the surface of rubber, which is essentially needed to be addressed in terms of gas−solid compatibility. However, the rubber used in power equipment is a polymer material with very complex molecular formula, and additives such as metal oxides are also added to the rubber to improve its sealing performance and reliability. This makes it difficult to analyze the specific reactions that occur between CF_3SO_2F gas and rubber. In this section, a brief analysis of the reaction mechanism will be conducted based on the experimental results.

The molecular formulas of EPDM and CR rubbers and CF_3SO_2F gas are shown in Figure 13. From the data in Tables 2−5, it can be seen that in addition to basic elements such as C and Cl, these rubbers also contain elements such as O, Zn, Mg, Al, Ca, etc., which are mainly from additives. Comparing the experimental group with the SF_6 control group, it can be seen that F will appear after the experiment in both EPDM and CR, and the proportion of F content increases with an increase of temperature. This indicates that CF_3SO_2F gas reacts with the rubber surface. For EPDM, there was no significant change in the C element and a slight decrease in the O element content, indicating that CF_3SO_2F may have reacted with the additives in it. For CR, there was a significant decrease in C element, indicating a reaction between the rubber body and the gas, which is consistent with the experimental test results. For the specific reaction process, further simulation calculation research is needed in the future.

CONCLUSIONS

In this study, the compatibility between CF_3SO_2F/N_2 mixed gas and commonly used EPDM and CR rubber materials is investigated experimentally. The conclusions are as follows.

(1) At the test temperatures of 70, 85, and 100 °C, the decomposition of CF_3SO_2F gas occurs after coexisting

https://doi.org/10.1021/acsomega.3c07958
ACS Omega 2024, 9, 7958−7966

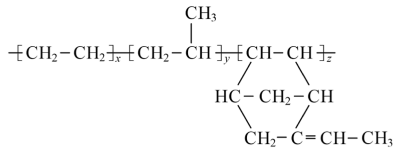

(a) Structural formula of EPDM rubber

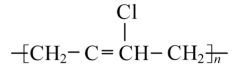

(b) Structural formula of CR rubber

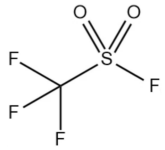

(c) Structural formula of CF_3SO_2F

Figure 13. Structural formulas of different rubbers and CF_3SO_2F gas.

with EPDM and CR for 7 d. The increase of temperature will lead to more serious decomposition of CF_3SO_2F gas. The mole proportion of CF_3SO_2F gas in the CF_3SO_2F/N_2 mixture will decreases accordingly. This is unfavorable for practical use, and it is necessary to focus on the changes in the mole proportion of CF_3SO_2F gas.

(2) The surface morphology of CR is degraded by CF_3SO_2F, and a large number of defects appear on the surface. The mechanical properties of CR are greatly affected by CF_3SO_2F. It means that CF_3SO_2F gas is incompatible with CR rubber, and CR is not suitable as a sealing material for equipment containing CF_3SO_2F gas. The change in EPDM surface morphology in CF_3SO_2F/N_2 is similar to that in SF_6. From this perspective, EPDM can be considered a sealing material for equipment containing CF_3SO_2F gas, but the temperature of the sealing ring needs to be strictly controlled, otherwise it will affect the performance of EPDM.

(3) The tensile property of EPDM and CR sealing rubber materials is less affected by temperature, but the compressive property is more affected by temperature, especially the PDC property. PDC and surface morphology are two more effective indicators for characterizing the compatibility between the insulating gas and rubber sealing materials. This provides a reference for future research on the gas−solid compatibility between other rubber sealing materials and EFI gases.

AUTHOR INFORMATION

Corresponding Authors

Yu Zheng − *State Key Laboratory of Power Grid Environmental Protection, Wuhan University, Wuhan 430072, China; School of Electrical Engineering and Automation, Wuhan University, Wuhan 430072, China;* orcid.org/0000-0002-9168-0683; Email: zywhuee@whu.edu.cn

Wenjun Zhou − *State Key Laboratory of Power Grid Environmental Protection, Wuhan University, Wuhan 430072, China; School of Electrical Engineering and Automation, Wuhan University, Wuhan 430072, China;* orcid.org/0000-0002-7532-9092; Email: wjzhou@whu.edu.cn

Authors

Wei Liu − *State Grid Anhui Electric Power Research Institute, Hefei 230000, China*

Wenliang Zhang − *China Electrotechnical Society, Beijing 100055, China*

Fengxiang Ma − *State Grid Anhui Electric Power Research Institute, Hefei 230000, China*

Zilin Tao − *State Key Laboratory of Power Grid Environmental Protection, Wuhan University, Wuhan 430072, China; School of Electrical Engineering and Automation, Wuhan University, Wuhan 430072, China*

Yuzheng Guo − *State Key Laboratory of Power Grid Environmental Protection, Wuhan University, Wuhan 430072, China; School of Electrical Engineering and Automation, Wuhan University, Wuhan 430072, China;* orcid.org/0000-0001-9224-3816

Complete contact information is available at: https://pubs.acs.org/10.1021/acsomega.3c07958

Notes

The authors declare no competing financial interest.

ACKNOWLEDGMENTS

The authors thank the National Key R&D Program of China (Grant no. 2021YFB2401400) and the State Grid Corporation of China Technology Project (Grant no. SGAHDK00LFJS2200332) for supporting this study and the Testing Center of Wuhan University for surface testing services.

REFERENCES

(1) Rabie, M.; Franck, C. M. Assessment of eco-friendly gases for electrical insulation to replace the most potent industrial greenhouse gas SF_6. *Environ. Sci. Technol.* **2018**, *52* (2), 369−380.

(2) Zhou, W. J.; Qiu, R.; Gao, K. L.; et al. Research Status of the Insulation Strength Prediction Models for the Eco-friendly Gases. *High Voltage Eng.* **2023**, *49* (03), 895−906.

(3) Smith, C.; Nicholls, Z. R. J.; Armour, K.; et al. *Climate Change 2021: The Physical Science Basis. Working Group I Contribution to the IPCC Sixth Assessment Report*; Cambridge University Press: Cambridge, United Kingdom and New York, NY, USA, IPCC, 2021.

(4) Li, C.; Zhang, L.; Wang, Y.; Yu, D.; Wang, Z.; Zhang, Z.; Connelly, L.; Lin, C.; Chen, G.; Mazzanti, G.; et al. Conductor Surface Rough-ness-dependent Gas Conduction Process for HVDC GIL-Part II: Ex-periment. *IEEE Trans. Dielectr. Electr. Insul.* **2021**, *28* (3), 988−995.

(5) Kieffel, Y.; Irwin, T.; Ponchon, P.; Owens, J. Green Gas to Replace SF_6 in Electrical Grids. *IEEE Power Energy Mag.* **2016**, *14* (2), 32−39.

(6) Long, Y. X.; Guo, L. P.; Wang, Y.; Chen, C.; Chen, Y.; Li, F.; Zhou, W. Electron swarms parameters in CF_3SO_2F as an alternative gas to SF_6. *Ind. Eng. Chem. Res.* **2020**, *59* (24), 11355−11358.

(7) Yu, X.; Hou, H.; Wang, B. A Priori Theoretical Model for Discovery of Environmentally Sustainable Perfluorinated Compounds. *J. Phys. Chem. A* **2018**, *122* (13), 3462−3469.

(8) Wang, Y.; Gao, Z.; Wang, B.; Zhou, W.; Yu, P.; Luo, Y. Synthesis and dielectric properties of trifluoromethanesulfonyl fluoride: an alternative gas to SF_6. *Ind. Eng. Chem. Res.* **2019**, *58* (48), 21913−21920.

https://doi.org/10.1021/acsomega.3c07958
ACS Omega 2024, 9, 7958−7966

(9) Hu, S.; Wang, Y.; Zhou, W.; Qiu, R.; Luo, Y.; Wang, B. Dielectric Properties of CF_3SO_2F/N_2 and CF_3SO_2F/CO_2 Mixtures as a Substitute to SF_6. *Ind. Eng. Chem. Res.* **2020**, *59* (35), 15796−15804.
(10) Zhang, B.; Zhang, Z.; Li, X.; Xiong, J.; Yang, T.; Deng, Y. The compatibility between environ-mentally friendly insulation gas C_4F_7N and α-Al2O3 (0001) surface: Theoretical and experimental insights. *Appl. Surf. Sci.* **2021**, *536*, 147839.
(11) Kessler, F.; Sarfert-Gast, W.; Kuhlmann, L.; Ise, M.; Heinemann, F. W. Compatibility of a Gaseous Dielectric with Al, Ag, and Cu and Gas-Phase Synthesis of a New N-Acylamidine Copper Complex. *Eur. J. Inorg. Chem.* **2020**, *2020* (20), 1989−1994.
(12) Li, Y.; Zhang, X.; Xiao, S.; Zhang, J.; Chen, D.; Cui, Z. Insight into the compatibility between C_4F_7N and silver: Experiment and theory. *J. Phys. Chem. Solids* **2019**, *126*, 105−111.
(13) Zheng, Z. Y.; Li, H.; Zhou, W. J.; et al. Compatibility of Eco-friendly Insulating Medium C_3F_7CN and Sealing Material EPDM. *High Voltage Eng.* **2020**, *46* (01), 335−341.
(14) Cheng, L.; Li, Y. L.; Zhang, X. X.; et al. Study on the Compatibility of EPDM and $C_5F_{10}O/CO_2$ Gas Mixture. *High Voltage Eng.* **2021**, *47* (05), 1771−1779.
(15) Lan, J. Q.; Tian, S. S.; Li, X. H.; et al. Compatibility between $C_6F_{12}O$-N_2 Gas Mixture and Sealing Material Nitrile Butadiene Rubber. *Trans. China Electrotechnical Soc.* **2022**, *37* (05), 1285−1293.
(16) Wu, P.; Ye, F. C.; Li, Y.; et al. Compatibility and Interaction Mechanism between $C_4F_7N/CO_2/O_2$ and EPDM. *Trans. China Electrotechnical Soc.* **2022**, *37* (13), 3393−3403.
(17) Wang, H.; Yan, X. L.; Han, D.; et al. Experiments for Compatibility Characteristics of C_4F_7N/CO_2 and Its Gas Byproducts with Commonly Used Rubber Sealing Materials. *High Voltage Eng.* **2022**, *48* (07), 2625−2634.
(18) Zhao, Y. H.; Qian, Y. H.; Chen, T. S.; et al. Experimental Study on SF_6 Gas Permeation Characteristics of Rubber Sealing Materials. *High Voltage Appar.* **2019**, *55* (10), 116−120.
(19) Rubber, vulcanized or thermoplastic—Determination of compression set - Part 1: At ambient or elevated temperatures. ISO 815−1, 2008.
(20) Rubber, vulcanized or thermoplastic—Determination of tensile stress-strain properties. ISO 37, 2005.
(21) Han, L.; Zheyu, Z.; Ruijun, Y.; et al. Compatibility between Gas and Solid Materials in Gas Insulated Equipment. *Trans. China Electrotechnical Soc.* **2020**, *35* (11), 2460−2468.
(22) Rubber—General procedures for preparing and conditioning test pieces for physical test methods. ISO 23529, 2004.
(23) High-voltage switchgear and controlgear—Part 1: Common specifications for alternating current switchgear and controlgear. IEC 62271-1, 2017.
(24) High-voltage switchgear and controlgear—Part 304: Classification of indoor enclosed switchgear and controlgear for rated voltages above 1 kV up to and including 52 kV related to the use in special service conditions with respect to condensation and pollution. IEC TS 62271-304, 2019.

https://doi.org/10.1021/acsomega.3c07958
ACS Omega 2024, 9, 7958−7966